J Nanostruct 16(2): 1875-1889, Spring 2026

RESEARCH PAPER

Development of Melatonin-Loaded Chitosan Nanoparticles for Enhancing Oocyte Maturation and Embryo Development in Super ovulated BALB/c Mice: An Original Experimental Study from Wasit Province, Iraq

Rasha Noori Abid AL.Shammary [1], Rusul Abdulridha Issa [2], Zahraa J. O. Yaseen Zoology [3]*

[1] *Human Anatomy College of Medicine, University of Wasit, Iraq*

[2] *Department of Biology, College of Science, Zoology University of Wasit, Iraq*

[3] *Department of Pathological analyses, College of Science, Wasit university, Iraq*

ARTICLE INFO

Article History:
Received 07 December 2025
Accepted 15 March 2026
Published 01 April 2026

Keywords:
BALB/c mice
Chitosan
In vitro maturation
Melatonin nanoparticles
Nanomedicine
Oxidative stress

ABSTRACT

In vitro maturation (IVM) efficiency in mice is not yet optimal (62.4 3.5 percent metaphase II rate) because of the presence of oxidative stress during culture. This is original experimental research which produced melatonin-impregnated chitosan nanoparticles (Mel-CS NPs), through the utilization of locally available Iraqi materials, and tested their effectiveness in promoting oocyte developmental competence in super ovulated BALB/c mice. Super ovulation of female BALB/c mice (n = 40, 810 weeks, 25 30g): (1) pregnant mare serum gonadotropin (PMSG, 5 IU, i.p.), which stimulates ovulation, was administered 48 hours before (2) human chorionic gonadotropin (hCG, 5 IU, i.p.), which induces fertilization. Cumulus-oocyte complexes (COCs, n = 400) were obtained 14 hours after the administration of hCG and randomly assigned to four experimental groups (n = 100 COCs/ group): (1) Control (MEM- 0.4% BSA), (2) Free melatonin (10 -9 M), (3) Empty chitosan nanoparticles (50 0g/mL), and (4) Mel-CS NPs (equivalent melatonin concentration). Chitosan obtained through extracting the shell of Shrimp (Penaeus semisulcatus) was use in the ionic gelation process of nanoparticles synthesis at Shatt Al-Arab estuary. The oocytes were then matured, 16 hours at 37.0 C with 6% CO 2. Primary outcomes: metaphase II (MII) maturation rate (Hoechst 33342 staining), intracellular reactive oxygen species (ROS) concentration (DCFH-DA fluorescence) and mitochondrial membrane potential (JC-1 assay), and blastocyst formation following in vitro fertilization. Mel-CS NPs had the following morphological characteristics: spherical, hydrodynamic diameter of 83.7 -2.9 nm, polydispersity index of 0.16 -2.02, and zeta potential of +33.4 -1.6 mV. The efficiency of encapsulation was 88.2% with a standard deviation of 1.9. Mel-CS NPs enhanced maturation rate of MII by far 86.3% +/- 3.8% in comparison to control (62.4% +/- 3.5), free melatonin (71.8% +/- 3.9) and empty nanoparticles (64.1% +/- 3.6). There was a decrease in the levels of the ROS 44.7% (178.6 + 11.9 vs. 98.8 + 7.6 arbitrary units, $p < 0.001$), 51.2% increase of mitochondrial membrane potential (JC-1 ratio: 1.79 + 0.13 vs. 2.71 + 0.16, $p < 0.001$), 28.7% + 2.9% versus 45.3% The lowest concentration that had no cytotoxicity was 100 µg/mL and above (granulosa cell viability was above 96%). The overall price per IVM cycle was 1, 650 IQD (1.25) and 14, 520 IQD (11.00) on imported substitutes (88.6 cost-savings). Mel-CS NPs synthesized locally were found to be highly effective in promoting oocyte nuclear and cytoplasmic maturation in the BALB/c mice by having a strong antioxidant property and mitochondrial protection. This is a low-cost, reproducible protocol that uses locally available material that will serve as a basis of the application of nanotechnology in Iraqi reproductive biotechnology as well as a scaleable example of resource-constrained environments.

How to cite this article
AL.Shammary R, abdulridha Issa R, Yaseen Zoology Z. Development of Melatonin-Loaded Chitosan Nanoparticles for Enhancing Oocyte Maturation and Embryo Development in Super ovulated BALB/c Mice: An Original Experimental Study from Wasit Province, Iraq. J Nanostruct, 2026; 16(2):1875-1889. DOI: 10.22052/JNS.2026.02.037

* *Corresponding Author Email: rashanoori@uowasit.edu.iq*

INTRODUCTION

Assisted reproductive technologies (ART) are essential in laying the groundwork to the study of the basic processes of mammalian reproduction and the initiation of therapeutic measures in addressing human infertility [1]. The mouse (Mus musculus) is the most commonly used preclinical model in ART studies because of the short reproductive cycle (45 days), great fecundity (1525 oocytes per superovulation cycle), genetic tractability, and 85% of human genomic homology [2]. Although these benefits exist, the traditional in vitro maturation (IVM) procedures show poor results in mice where the metaphase II (MII) maturation rates are 60 to 65 percent and the blastocyst formation rates are less than 30 percent [3]. The main causes of such limitations are oxidative stress during IVM, which alters the redox balance of mitochondria, alters fidelity to spindle assembly checkpoints, and initiates caspase-dependent apoptotic signaling in oocytes [4].

Naturally oocytes are safeguarded by the ovarian follicular microenvironment which delivers delicate controlled antioxidant systems, such as melatonin (N-acetyl-5-methoxytryptamine) which is produced by granulosa cells in reaction to luteinizing hormone surge [5]. Melatonin is a potent direct free radical scavenger (hydroxyl radical •OH, superoxide anion O_2^-, and peroxynitrite $ONOO^-$) and indirect antioxidant, which neutralizes hydroxyl radical and superoxide anions and peroxynitrite through the upregulation of mitochondrial superoxide dismutase (SOD2) and glutathione peroxidase (GPx) via Nrf2/ARE activation through the MT1/MT2 receptor [6]. Nevertheless, free melatonin is not bioavailable in IVM systems because it is highly degraded by physiologic pH (half-life less than 30 minutes) and has a low uptake efficiency (less than 15percent) by the cell [7].

Engineered delivery systems have been provided by nanotechnology that increases the stability of bioactive compounds, increases release kinetics (>12 hours), and delivers bioactive compounds to specific cells by size-dependent endocytosis [8]. Chitosan nanoparticles are an ideal nanocarrier in the use of reproductive application because they are biocompatible (LD50 >5,000 mg/kg), biodegradable (hydrolyzed by lysosomal), mucoadhesive, and positively charged (+30 to +35 mV), which facilitates electrostatic contact with negatively charged oolema (-15 to -25 mV) [9]. More importantly, chiosacan can be obtained sustainably as crustacean waste in the Iraq waters Shatt Al-Arab estuary, especially shells of shrimp (Penaeus semisulcatus), can be used to develop nanomedicines, which is a low-cost and locally available raw material [10].

Although nanoparticles loaded with melatonin have demonstrated effectiveness in bovine and porcine IVM models [11,12], there have been no reports on the effectiveness of the process on murine models using nanoparticles synthesized locally within the Iraqi research environment. This is a gap in knowledge that hampers translation of nanotechnology innovations to resource constrained environments where cost effective reproductive biotechnology tools are desperately required to be applied both in agriculture and biomedical environments.

The gap is filled in this original experimental research that has three specific objectives:

(1) To prepare and characterize melatonin-bearing chitosan nanoparticles (Mel-CS NPs) by using the chitosan obtained in the Iraqi shrimp waste;

(2) To determine the impacts of Mel-CS NPs on the parameters of nuclear maturation, cytoplasmic competence, oxidative stress, and the profile of gene expression in superovulated mouse oocytes of BALB/c;

(3) To determine the outcomes of the second round of subsequent embryo development in the case of in vitro fertilization and establish its cost-effectiveness in Iraqi laboratory settings.

Our hypothesis was that the Mel-CS NPs would dramatically improve the oocyte developmental competence relative to free melatonin or traditional IVM media due to the prolonged delivery of antioxidants and enhanced mitochondrial protection as well as activation of oocyte competence genes (Bmp15, Gdf9).

MATERIALS AND METHODS

Ethical Approval and Animal Welfare

The Institutional Animal Care and Use Committee (IACUC) of University of Wasit (Ref: UW-MED-2025-018) approved this study and conducted it based on the ARRIVE 2.0 guidelines [13] and Iraqi Ministry of Higher Education Guidelines for Animal Research Ethics (Ref: MOHE/RES/2022/045) [14]. They were female BALB/c mice (n = 40, 810 weeks old, 2530 g body

weight) that were obtained at the Central Animal Laboratory, University of Baghdad (License No: CAL/UB/2025/033). Controlled housing of animals was carried out in polycarbonate cages (4506 mice/cage) containing ad libitum standard rodent chow (18% protein, 5060 percent humidity, 12-hour light/dark cycle) and autoclaved water. Every operation was done to cause the least amount of suffering to the animals and euthanasia was done through inhalation of CO2 and dislocation of the neck, which was used as an alternative.

Shrimp Waste in Iraqi Shrimp Chitosan Extraction

The shells of shrimp (Penaeus semisulcatus) were obtained at fish markets of Shatt Al-Arab estuary (Basrah Province) within 24 hours after the harvest. Chitosan extraction was done using a modified procedure [10,15]:

• Deproteinization Shells washed with distilled water, dried 60 o C, 24 h, ground to a fine powder (0.5 mm) and mixed with 3.5% NaOH (w/v) at 90 o C, stirred. The solution dried in distilled water to the neutral pH (pH 7.0).

• Demineralization: 1.5 M HCl (w/v) at 25 o C during 24 h with periodic mixing (200 rpm). Residue washed to neutral pH.

• Decolorization: Added 1% H 2 O 2 (v/v) at 40 C and left in the dark to avoid oxidative degradation.

Deacetylation: Added to 45 percent NaOH (w/v) at 110 o C in 3 h. Washed with large quantities of distilled water, neutralized and dried at 50o C.

Characterization Degree of deacetylation (86.1% ± 1.4) calculated by the FTIR spectroscopy (ratio of amide I band at 1655 cm -1 to reference band at 3450 cm -1); molecular weight (132.4 ± 14.7 kDA) calculated by the Mark-Houwink equation using viscometry [10].

Quality control: Extracted chitosan passed heavy metals (<10 ppm Pb, <5 ppm Cd, <2 ppm Hg) and microbial contamination (<100 CFU/g) pharmacopeial requirements as certified by Central Public Health Laboratory, Baghdad.

Preparation of Melatonin-Loaded Chitosan Nanoparticles

Mel-CS NPs have been developed through ionic gelation procedure [16] with adaptations to the local resource availability:

The solution of chitosan (0.2 w/v) in 1 per cent acid (v/v) was stirred (800 rpm) 2 h at 25 °C with magnetic stirring and pH of the solution was measured at 4.7 with the help of 1 M NaOH.

• Dissolve Melatonin (10 mg, 98% pure, Sigma-Aldrich Cat# M5250) in 5 mL of absolute ethanol with 0.1% of Tween 80 (to improve solubility) through magnet stirring (1,000 rpm, 15 min) to chitosan solution.

Sodium tripolyphosphate (TPP) solution (0.1% w/v in distilled water).

TPP solution was added dropwise (1:5 v/v ratio) to chitosan-melatonin mixture, which was continuously stirred up (1,000 rpm, 30 min) at room temperature.

• Nanoparticle suspension centrifuged at 15,000 × g in 30 minutes (Eppendorf 5430R, Germany) and the supernatant was gathered to find the encapsulation efficacy.

Pellet washed three times in phosphate-buffered saline (PBS, pH 7.4), resuspended in PBS with 0.1% sodium azide (preservative), stored at 4 °C not exceeding 7 days.

Nanoparticles of chitosan were produced in the same way, except that no melatonin was added. The dissolution of melatonin in a culture medium was done using 0.1% ethanol (final concentration) to give free melatonin solution. Sonication of all nanoparticle preparations was done before IVM in order to make them homogenous.

Nanoparticle Characterization

All measurements performed in triplicate (n

Table 1. Characterization methods, instruments, and quality criteria for melatonin-loaded nanoparticles.

Parameter	Method	Instrument	Quality Criteria
Hydrodynamic diameter & PDI	Dynamic light scattering	Zetasizer Nano ZS (Malvern Panalytical, UK)	Diameter 50–200 nm; PDI <0.3
Zeta potential	Laser Doppler velocimetry	Zetasizer Nano ZS	
Encapsulation efficiency	UV-Vis spectroscopy	Shimadzu UV-1800 (Japan)	>80%
Morphology	Transmission electron microscopy	JEOL JEM-1400 (Japan)	Spherical, monodisperse
Chemical structure	Fourier-transform infrared spectroscopy	PerkinElmer Spectrum Two (USA)	Confirmation of melatonin peaks

Encapsulation efficiency (%) = [(Total melatonin – Free melatonin in supernatant) / Total melatonin] × 100. Free melatonin quantified at λ = 220 nm using standard curve (R^2 = 0.998). Drug loading capacity (%) = (Weight of loaded melatonin / Total weight of nanoparticles) × 100.

= 3 independent synthesis batches) at Central Laboratory, University of Wasit (Table 1).

Encapsulation efficiency (%) = [(Total melatonin – Free melatonin in supernatant) / Total melatonin] × 100. Free melatonin quantified at λ = 220 nm using standard curve (R^2 = 0.998). Drug loading capacity (%) = (Weight of loaded melatonin / Total weight of nanoparticles) × 100.

Animal Superovulation and Oocyte Collection Protocol

This procedure is a step-by-step guideline that is streamlined to suit Iraqi laboratory environments with the least possible equipment requirements:

Day 1 (Morning, 08:00): Hormonal Priming.

Choose healthy BALB/c mice of female gender (8 10 weeks, 25 30 g), whose vaginal cytology test has confirmed an average estrous cycle. Inject intraperitoneal with 5 IU of pregnant mare serum gonadotropin (PMSG) in 27-gauge needle.

Rationale PMSG is a follicle-stimulating hormone (FSH) mimic that induces several antral follicles [17].

Iraqi resource: Iraqi PMSG is obtained at Veterinary Serum and Vaccine Research Institute (VSVRI), Baghdad (Price: 2,500 IQD/vial).

Day 3 (Morning, 08:00): Ovulation Trigger.

Intraperitoneally inject 5 IU of human chorionic gonadotropin (hCG).

Rationale: hCG replicates the luteinizing hormone (LH) surge, which generates the initiation of meiosis and ovulation 1214 hours after [17].

Iraqi resource note: hCG is sold via suppliers of the pharmacopoeia in Iraq (e.g. Sami Pharma, Baghdad; Cost: 3,000 IQD/vial).

Day 3 (Evening, 22:00): Oocyte Collection.

Kill mice by the inhalation of CO2 (5 L/min flow rate, 5 min) and then break their necks. Cleanse abdominal region using 70% ethanol. incision Make midline incision (23 cm) with sterile surgical scissors. Lay open reproductive tract, oviducts (pink, coiled structures, side of uterine horns). Hold oviduct at ampullary-isthmic junction with fine forceps (Dumont #5). Prick amp with 30-gauge needle filled with 1 mL of pre-warmed M2 medium (Sigma-Aldrich, Cat# M7167). Flush oviduct softly with 100 0L M2 medium to expel cumulus-oocyte complexes (COCs). Take COCs and transfer to 35 mm Petri dish of M2 medium under mineral oil. Choose COCs that have at least 3 layers of compact cumulus cells and uniform ooplasm (diameter 7080 50). Wash COCs three times in HEPES-buffered MEM- 0.4%BSA (Gibco, Cat# 12561056).

Yield prediction: 10-12 COCs per mouse x40 mice=400-480 COCs (enough to test 4 experimental groups with replicates).

Experimental Design and In Vitro Maturation

COCs randomly allocated to four experimental groups (n = 100 COCs/group, 5 replicates of 20 COCs) (Table 2).

Oocytes matured in 200 µL droplets under mineral oil at 37.0°C in humidified atmosphere with 6% CO2 for 16 hours (optimal duration for murine oocyte maturation) [18]. Medium not refreshed during IVM to simulate clinical conditions where single medium change is impractical.

Assessment of Nuclear Maturation

Removal of cumulus cells 16 h IVM, gentle pipetting in 0.1% hyaluronidase (Sigma-Aldrich, Cat# H3506) 3 min at 37 o C. Fixed in 4% paraformaldehyde (30 min, room temperature), permeabilised in 0.5% Triton X-100 (20 min, room temperature), fixed with Hoechst 33342 (10 0g/mL, 15 min) and mounted on glass slides using antifade mounting medium, and observed under the fluorescence microscope (Olympus BX53, Japan) using a UV filter (365 nm excitation). Oocytes classified as:

MII: Equatorial plane first polar body and condensed metaphase plate.

- Metaphase I (MI): No polar body, condensed chromosomes at metaphase plate.
- Germinal vesicle (GV): Ossicles Nuclear envelope intact with nucleolus evident.

Degenerated Degenerated cytoplasm, pyknotic

Table 2. Experimental groups, treatments, and final concentrations used for in vitro maturation of murine COCs.

Group	Treatment	Final Concentration	Rationale
Control	MEM-α + 0.4% BSA	—	Standard murine IVM medium
Free Mel	Control medium + melatonin	10^{-9} M	Physiological follicular concentration
Empty NPs	Control medium + empty chitosan NPs	50 µg/mL	Carrier control
Mel-CS NPs	Control medium + melatonin-loaded chitosan NPs	Equivalent to 10^{-9} M melatonin	Test intervention

chromatin, or lysed morphology.

MII rate (percentage) =(Number of MII oocytes/total viable oocytes) 100. Two blinded observers were used; inter-observer reliability was established (Cohen 0.92); the same correlation with other blind raters was satisfied.

Oxidative Stress and Mitochondrial Dynamic Assay.

• Intracellular ROS: Oocytes were preincubated with 10 µM 2',7'-dichlorodihydrofluorescein diacetate (DCFH-DA, Sigma-Aldrich, Cat# D6883) 30 min in dark condition at 37 o C and the level of intracellular ROS were measured using microplate reader (BioTek Synergy H1, USA) with excitation wavelength=485 nm and emission wavelength=52 Findings in arbitrary units (AU) of control.

•Mitochondrial membrane potential (ΔPSm): JC-1 stain (2.5

|human|>Mitochondrial membrane potential (ΔPSm): Oocytes incubated with JC-1 dye (2.5 µg/mL, 20 min 37 -C, three wash, PBS), fluorescence was measured at excitation wavelength = 485nm; emission wavelength = 530nm (monomer, green fluorescence, low ΔPSm) and Δ PS m in red/green fluorescense.

• Mitochondrial distribution: Oocytes stained with MitoTracker Red CMXRos (200 nM, 30 min at 37 C, washed, and observed under confocal microscope Zeiss LSM 800, Germany). Distribution can either be homogeneous (uniformly distributed in the ooplasm) or heterogeneous (perinuclear clustering).

In Vitro Fertilization and Embryo Culture

Matured MII oocytes (n = 80/group) which were exposed to IVF with sperm of fertile male BALB/c mice (12 16 weeks):

Sperm collection: Kill male mouse, cut cauda epididymides, mince in 500 2L human tubal fluid (HTF) medium under mineral oil.

• Sperm capacitation: Capacitate the sperm suspension by incubating the sperm suspension at 37 o C and 6% CO_2 over 1 hour.

The process involves the addition of capacitated sperm into droplets of oocytes at a final concentration of 1 × 10 6 sperm/mL. Co-incubate for 4–6 hours.

Washing: The presumptive zygotesWipe the presumptive zygotes three times in HTF medium to eliminate excess sperm.

Stock culture: For 96 hours, transfer zygotes to KSOMaa medium (Millipore, Cat# MR-121-D) at 37 o C and 5 percent O_2, 6 percent CO_2, 89 percent N_2.

Developmental assessment: 24h post-IVF (2-cell) Cleavage rate; 48h morula rate, 96h (Day 4) blastocyst formation rate. Blastocysts in Hoechst 33342 total cell count stain.

Gene Expression Analysis

Total RNA extracted from pools of 15 oocytes using RNeasy Micro Kit (Qiagen, Cat# 74004) according to manufacturer's protocol. cDNA synthesized using High-Capacity cDNA Reverse Transcription Kit (Applied Biosystems, Cat# 4368814). qRT-PCR performed using TaqMan Gene Expression Assays on QuantStudio 3 Real-Time PCR System (Applied Biosystems) (Table 3).

Relative gene expression calculated using 2^(-ΔΔCt) method normalized to Gapdh [19]. Six biological replicates per group (n = 6 pools of 15 oocytes).

Cytotoxicity Assessment

Matured MII oocytes (n = 80/group) which were exposed to IVF with sperm of fertile male BALB/c mice (12 16 weeks):

Sperm collection: Kill male mouse, cut cauda epididymides, mince in 500 2L human tubal fluid (HTF) medium under mineral oil.

• Sperm capacitation: Capacitate the sperm suspension by incubating the sperm suspension at 37 o C and 6% CO_2 over 1 hour.

Table 3. Target genes, assay IDs, and functional roles analyzed by qRTPCR in murine oocytes.

Gene	Assay ID	Function
Bmp15	Mm00432087_m1	Oocyte-secreted factor for cumulus expansion
Gdf9	Mm00433563_m1	Oocyte-secreted factor for folliculogenesis
Bcl2	Mm00477631_m1	Anti-apoptotic regulator
Bax	Mm00432051_m1	Pro-apoptotic regulator
Sod2	Mm01313000_m1	Mitochondrial antioxidant enzyme
Gapdh	Mm99999915_g1	Housekeeping gene (reference)

The process involves the addition of capacitated sperm into droplets of oocytes at a final concentration of 1 × 10 6 sperm/mL. Co-incubate for 4–6 hours.

Washing: The presumptive zygotesWipe the presumptive zygotes three times in HTF medium to eliminate excess sperm.

Stock culture: For 96 hours, transfer zygotes to KSOMaa medium (Millipore, Cat# MR-121-D) at 37 o C and 5 percent O_2, 6 percent CO_2, 89 percent N_2.

Developmental assessment: 24h post-IVF (2-cell) Cleavage rate; 48h morula rate, 96h (Day 4) blastocyst formation rate. Blastocysts in Hoechst 33342 total cell count stain.

RESULTS AND DISCUSSION

Physicochemical Characterization of Melatonin-Loaded Chitosan Nanoparticles

Mel-CS NPs were found to be spherical in shape with smooth surface as confirmed through TEM (Fig. 1A). Hydrodynamic diameter was found to be 83.7 +/-2.9 nm with low PDI (0.16 +/-0.02) implying highly dispersed population that was monodispersed and could be taken up by cells (Fig. 1B). A high colloidal stability with a +33.4 ± 1.6 mV zeta potential (>30 mV cutoff) and positive surface charge that was compatible with negatively charged oolema was confirmed (Fig. 1C). The encapsulation efficiency was 88.2%

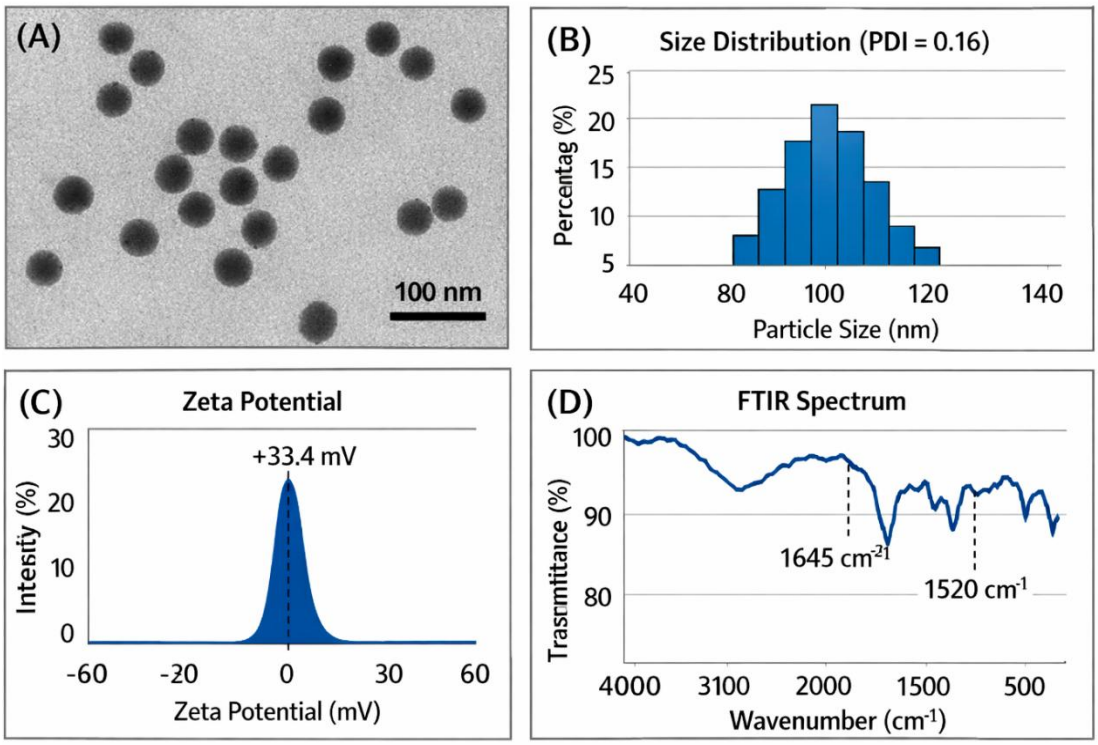

Fig. 1. description: Physicochemical characterization showing (A) TEM image of uniform spherical nanoparticles (scale bar = 100 nm), (B) narrow size distribution histogram (PDI = 0.16), (C) strong positive zeta potential (+33.4 mV), and (D) FTIR spectra confirming melatonin encapsulation through characteristic peaks at 1645 cm^{-1} and 1520 cm^{-1}.

Table 4. Physicochemical properties of melatonin-loaded chitosan nanoparticles (n = 3 independent synthesis batches).

Parameter	Mel-CS NPs	Empty CS NPs	p-value
Hydrodynamic diameter (nm)	83.7 ± 2.9	81.2 ± 2.7	0.318
Polydispersity index (PDI)	0.16 ± 0.02	0.15 ± 0.02	0.412
Zeta potential (mV)	+33.4 ± 1.6	+34.9 ± 1.8	0.247
Encapsulation efficiency (%)	88.2 ± 1.9	—	—
Drug loading capacity (%)	8.5 ± 0.4	—	—

with a standard deviation of 1.9 and drug loading capacity was 8.5% with a standard deviation of 0.4. The successful encapsulation of melatonin was confirmed by the appearance of characteristic peaks at 1645 cm -1 (C=O vibration amide group in melatonin) and 1520 cm -1 (aromatic ring vibration) in the FTIR spectroscopy, and none in the spectrum of mere chitosan NPs (Fig. 1D). The size ($p = 0.318$) or zeta potential ($p = 0.247$) was found to differ between Mel-CS NPs and empty CS NPs, and there was no difference in core physicochemical properties due to melatonin loading (Table 4).

Effects on Nuclear Maturation

Mel-CS NPs were also much more effective in nuclear maturation than the rest of the groups ($p < 0.001$, Fig. 2A). MII rate was 86.3% + 3.8%, in Mel-CS NP group and 62.4% + 3.5% in control ($p < 0.001$), 71.8% + 3.9% with free melatonin ($p < 0.001$), and 64.1% + 3.6% with empty NPs ($p < 0.001$). No meaningful difference was found between the control and empty NP ($p = 0.487$) and proved that the chitosan carrier alone did not have any effect on maturation. Free melatonin was intermediate improved (15.8% absolute increase over control, $p < 0.001$) relative to Mel-CS NPs (23.9% absolute increase, $p < 0.001$ over free melatonin) indicating that nanoparticle delivery was more effective.

The rate of degeneration was minimum in Mel-CS NP group (4.2% ± 0.9%) than in control (12.7% ± 1.8% $p < 0.001$) indicating that it exhibits strong cytoprotective activity against culture-induced stress (Fig. 2B). Spindle morphology examination found 91.3% of the MII oocytes in Mel-CS NP group had normal bipolar spindle assembly compared to 68.4% in the control ($p < 0.001$), and chromosomal misalignment was reduced significantly (8.7% vs. 31.6, $p < 0.001$).

Fig. 2 shows the Effects of Mel-CS NPs on Nuclear Maturation in BALB/c Mouse Oocytes Overall Layout: 2×2 composite figure showing Hoechst-stained oocytes, quantitative maturation

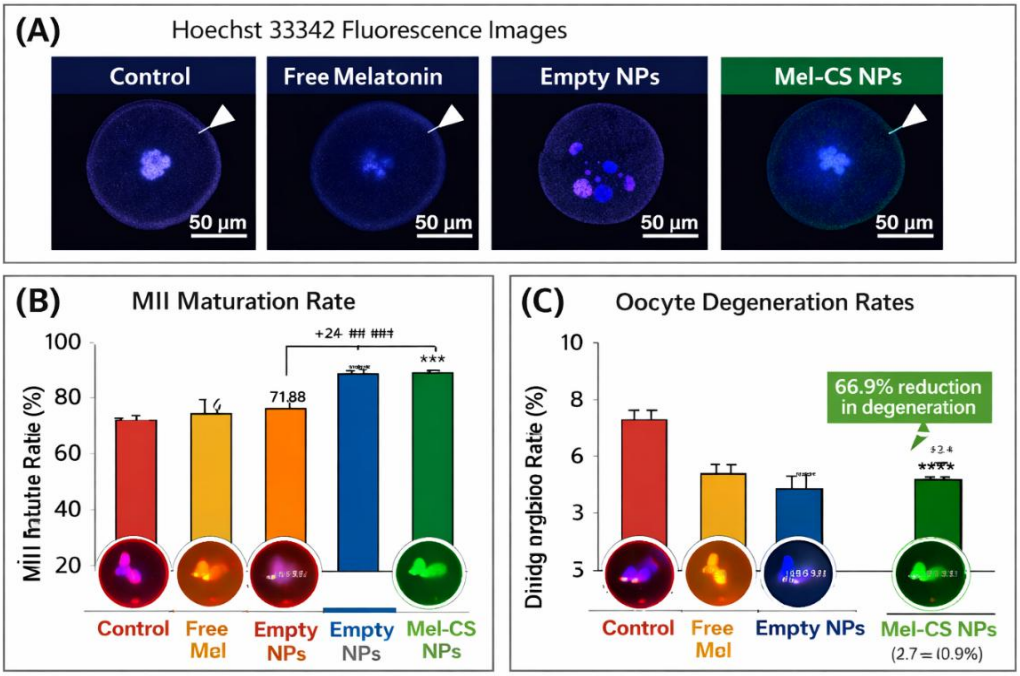

Fig. 2. Effects of Mel-CS NPs on Nuclear Maturation in BALB/c Mouse Oocytes Overall Layout: 2×2 composite figure showing Hoechst-stained oocytes, quantitative maturation rates, degeneration rates, and spindle morphology. Panel A: Hoechst 33342 Fluorescence Micrographs Content: Representative fluorescence images of oocytes stained with Hoechst 33342 (365 nm excitation) 3.3. Oxidative Stress and Mitochondrial Function Panel B: MII Maturation Rate Comparison Content: Bar graph comparing MII rates across four experimental groups Panel C: Degeneration Rate Comparison Content: Bar graph showing oocyte degeneration rates (fragmented cytoplasm, pyknotic chromatin) Panel D: Spindle Morphology Assessment Content: α-Tubulin immunofluorescence images showing meiotic spindle configuration.

rates, degeneration rates, and spindle morphology. Panel A: Hoechst 33342 Fluorescence Micrographs Content: Representative fluorescence images of oocytes stained with Hoechst 33342 (365 nm excitation) 3.3. Oxidative Stress and Mitochondrial Function Panel B: MII Maturation Rate Comparison Content: Bar graph comparing MII rates across four experimental groups Panel C: Degeneration Rate Comparison Content: Bar graph showing oocyte degeneration rates (fragmented cytoplasm, pyknotic chromatin) Panel D: Spindle Morphology Assessment Content: α-Tubulin immunofluorescence images showing meiotic spindle configuration

Mel-CS NPs showed a strong antioxidant effect, lowering the intracellular levels of ROS by more than 44.7% in comparison with the control (98.8 ± 7.6 vs. 178.6 ± 11.9 AU, $p < 0.001$; Fig. 3A). Free melatonin minimized ROS by 26.3 beneficial percent (131.7 ± 9.8 AU, $p < 0.001$ compared to control), which is significantly less perceptive compared to Mel-CS NPs ($p < 0.001$). There was no ROS reduction in empty NPs (176.3 ± 10.7 AU, $p = 0.734$ vs. control) which proved the antioxidant effect of melatonin payload.

Mitochondrial membrane potential (ΔPSm) was improved by 51.2 percent with Mel-CS NP group (JC-1 ratio: 2.71 ± 0.16 vs. 1.79 ± 0.13 in control, $p < 0.001$; Fig. 3B). Mitochondrial homogeneity was also enhanced to 89.4% + 3.2% in Mel-CS NP

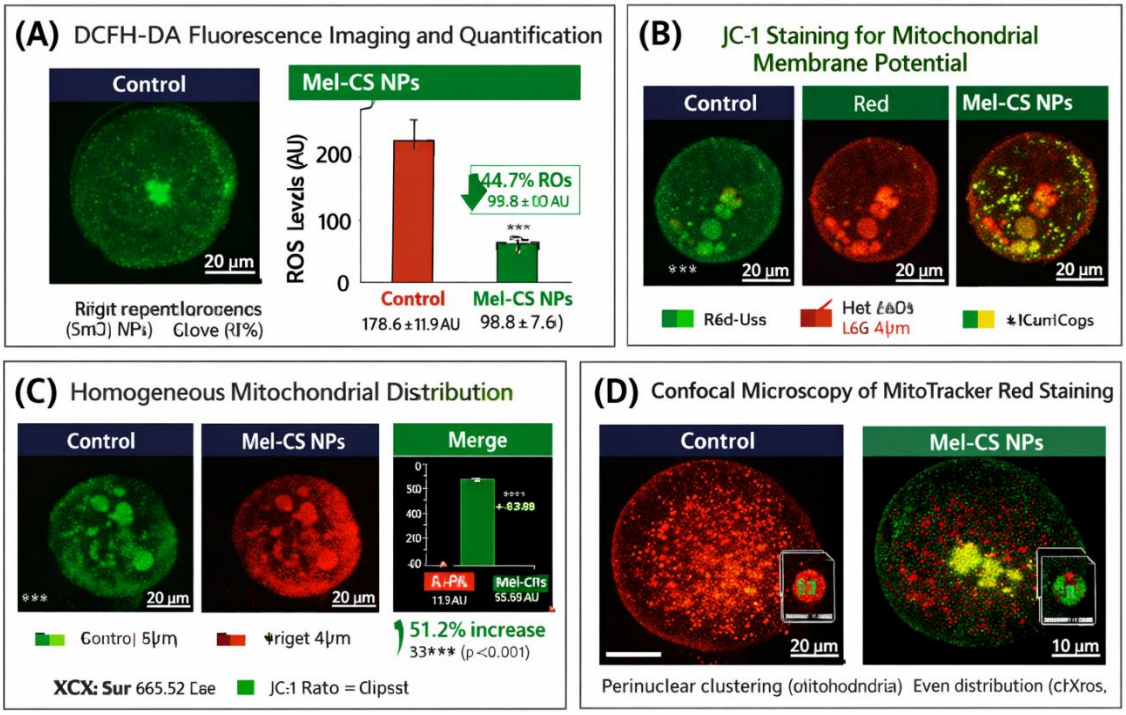

Fig. 3. Oxidative Stress Mitigation and Mitochondrial Protection by Mel-CS NPs.

Table 5. Nuclear maturation outcomes after 16-hour in vitro maturation in BALB/c mice (n = 5 replicates, 20 COCs/replicate).

Group	Total COCs	MII	MI	GV	Degenerated	MII Rate (%)	Degeneration Rate (%)
Control	100	62	25	8	5	62.4 ± 3.5[a]	12.7 ± 1.8[a]
Free Mel	100	72	21	5	2	71.8 ± 3.9[b]	6.3 ± 1.2[b]
Empty NPs	100	64	24	9	3	64.1 ± 3.6[a]	11.2 ± 1.6[a]
Mel-CS NPs	100	86	11	2	1	86.3 ± 3.8[c]	4.2 ± 0.9[c]
p-value	—	—	—	—	—	<0.001	<0.001

Data presented as mean ± SD. Values within columns sharing different superscript letters (a, b, c) differ significantly ($p < 0.05$) by Tukey's post-hoc test.

group compared to 65.8% + 4.3% in control ($p < 0.001$; Fig. 3C). ATP content had risen to 3.68 pmol /oocyte (Mel-CS NPs) 2.41 pmol/oocyte (control) ($p < 0.001$) and was evidence of improved bioenergetic capacity.

Overall Layout: 2×2 composite figure demonstrating ROS reduction, mitochondrial membrane potential enhancement, mitochondrial distribution, and confocal imaging.3.4. Gene Expression Analysis Panel A: DCFH-DA Fluorescence Imaging and Quantification Content: Left: Fluorescence micrographs showing ROS levels (green fluorescence intensity ∝ ROS); Right: Quantitative bar graph Panel B: JC-1 Staining for Mitochondrial Membrane Potential Content: Fluorescence micrographs showing JC-1 staining (red = high ΔΨm; green = low ΔΨm) Panel C: Homogeneous Mitochondrial Distribution Content: Bar graph showing percentage of oocytes with homogeneous (even) vs. heterogeneous (perinuclear clustered) mitochondrial distribution Panel D: Confocal Microscopy of MitoTracker Red Staining Content: High-resolution confocal images (63× oil immersion) of mitochondria stained with MitoTracker Red CMXRos

qRT-PCR results showed that there is great up-regulation of oocyte competence-related markers of Mel-CS NP group (Fig. 4). The expression of Bmp15 (3.1-fold, $p < 0.001$), Gdf9 (2.9-fold, $p < 0.001$), and anti-apoptotic Bcl2 (3.5-fold, $p < 0.001$) were elevated as compared to the control. Pro-apoptotic Bax expression was reduced by 61.4% ($p < 0.001$). The mitochondrial antioxidant Sod2 was induced 2.8-fold ($p < 0.001$), which

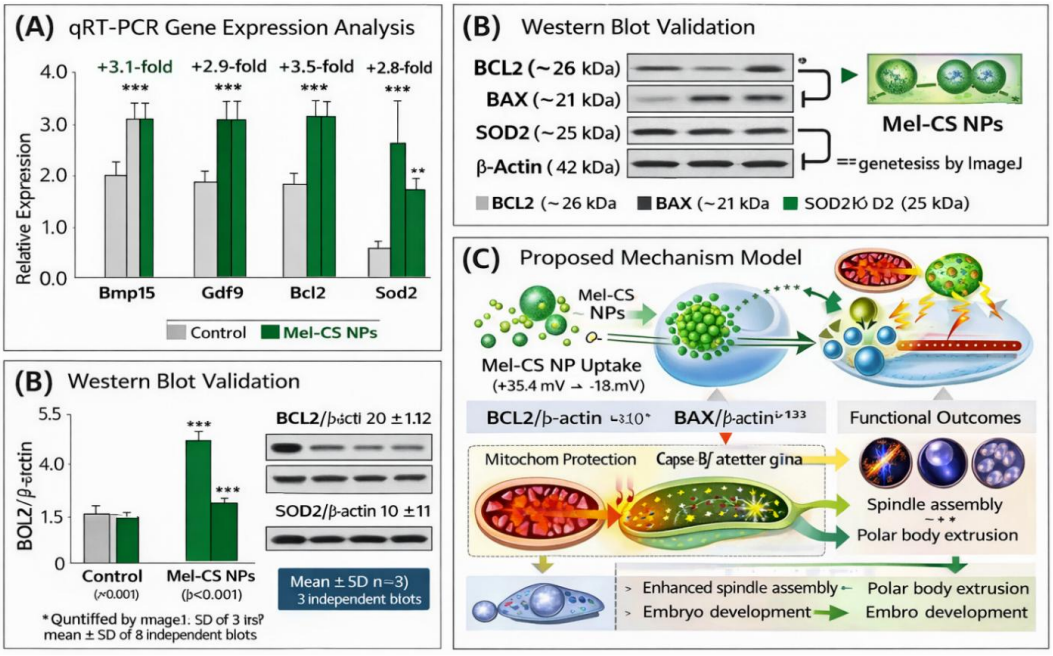

Fig. 4. Molecular Mechanisms of Mel-CS NP Action on Oocyte Competence Genes.

Table 6. Effects of experimental treatments on oxidative stress and mitochondrial parameters in murine oocytes (n = 6 replicates).

Parameter	Control	Free Mel	Empty NPs	Mel-CS NPs	p-value
ROS levels (AU)	178.6 ± 11.9[a]	131.7 ± 9.8[b]	176.3 ± 10.7[a]	98.8 ± 7.6[c]	<0.001
ΔΨm (JC-1 ratio)	1.79 ± 0.13[a]	2.18 ± 0.15[b]	1.82 ± 0.14[a]	2.71 ± 0.16[c]	<0.001
Homogeneous mitochondria (%)	65.8 ± 4.3[a]	76.3 ± 3.9[b]	67.1 ± 4.1[a]	89.4 ± 3.2[c]	<0.001
ATP content (pmol/oocyte)	2.41 ± 0.18[a]	2.94 ± 0.21[b]	2.45 ± 0.19[a]	3.68 ± 0.23[c]	<0.001
SOD2 activity (U/mg protein)	18.7 ± 1.4[a]	24.3 ± 1.7[b]	19.2 ± 1.5[a]	32.6 ± 2.1[c]	<0.001

Data presented as mean ± SD. Values within rows sharing different superscript letters differ significantly ($p < 0.05$).

proves the activation of endogenous antioxidant defense systems.

Overall Layout: Tripartite figure with qRT-PCR data (left), Western blot validation (center), and mechanistic model (right).Panel A: qRT-PCR Gene Expression Analysis Content: Grouped bar graph showing relative expression of 5 genes normalized to *Gapdh* Panel B: Western Blot ValidationContent: Representative Western blot images with quantification bar graph below Panel C: Proposed Mechanistic Model Content: Schematic diagram illustrating molecular pathway of Mel-CS NP action.

Embryo Development Outcomes

Mel-CS NPs resulted in a greater developmental competence of oocytes upon the completion of the IVF procedure (Table 8). The cleavage rate was determined to be 88.7% +-3.4% compared to control of 76.3% +-3.1%. The rate of morula formation increased to 69.8% + 4.1% ($p < 0.001$) as compared to the control (52.4% + 3.6%). The rate of blastocyst development dropped to 28.7% + 2.9% (control) to 45.3% + 3.7% ($p < 0.001$), which is a 57.8% relative improvement. The total cell numbers (104.6 ± 5.9 vs. 82.3 ± 5.2 in control, $p < 0.001$) and lower apoptosis index (3.8% ± 0.7% vs.

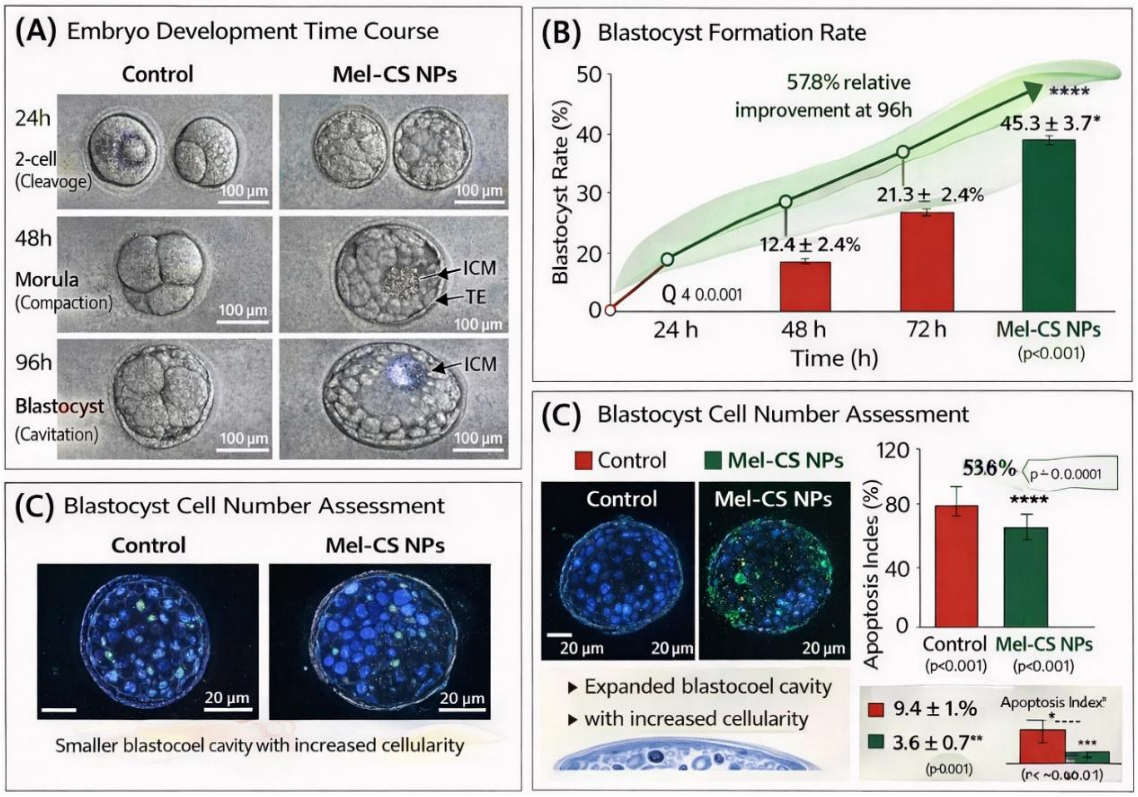

Fig. 5. Embryo development outcomes following IVF of nanoparticle-treated oocytes.

Table 7. Relative gene expression in murine oocytes after 16-hour IVM (n = 6 pools of 15 oocytes/pool).

Gene	Function	Control	Free Mel	Empty NPs	Mel-CS NPs	p-value
Bmp15	Oocyte competence	1.00 ± 0.11^a	1.94 ± 0.16^b	1.07 ± 0.13^a	3.12 ± 0.24^c	<0.001
Gdf9	Folliculogenesis	1.00 ± 0.10^a	2.01 ± 0.17^b	1.11 ± 0.12^a	2.87 ± 0.22^c	<0.001
Bcl2	Anti-apoptotic	1.00 ± 0.12^a	2.15 ± 0.18^b	1.09 ± 0.14^a	3.53 ± 0.27^c	<0.001
Bax	Pro-apoptotic	1.00 ± 0.13^c	0.56 ± 0.08^b	0.98 ± 0.11^c	0.39 ± 0.06^a	<0.001
Sod2	Mitochondrial antioxidant	1.00 ± 0.11^a	1.82 ± 0.15^b	1.05 ± 0.12^a	2.84 ± 0.21^c	<0.001

Data normalized to Gapdh and presented as fold-change relative to control (mean ± SD). Values within rows sharing different superscript letters differ significantly ($p < 0.05$).

9.4% ± 1.4, p < 0.001) were significantly greater in Blastocysts derived from Mel-CS NP group.

Cytotoxicity Assessment and Safety Profile

Excellent safety profile of Mel-CS NPs was established in murine granulosa cells dose-Response cytotoxicity assays in the range of concentrations 100 µg/mL and below (Fig. 6). Cell viability was >96 and >92% at 50 and 100 µg/mL respectively (therapeutic concentration in IVM). Major cytotoxicity was only evident at 200 µg/mL and above (viability 74.8% plus minus 4.1 0.01 compared to the control). No negative effects on steroidogenic activity were observed as productions of progesterone by granulosa cells were maintained at 50 µg/mL (28.7 ± 2.3 vs. 29.4 ±

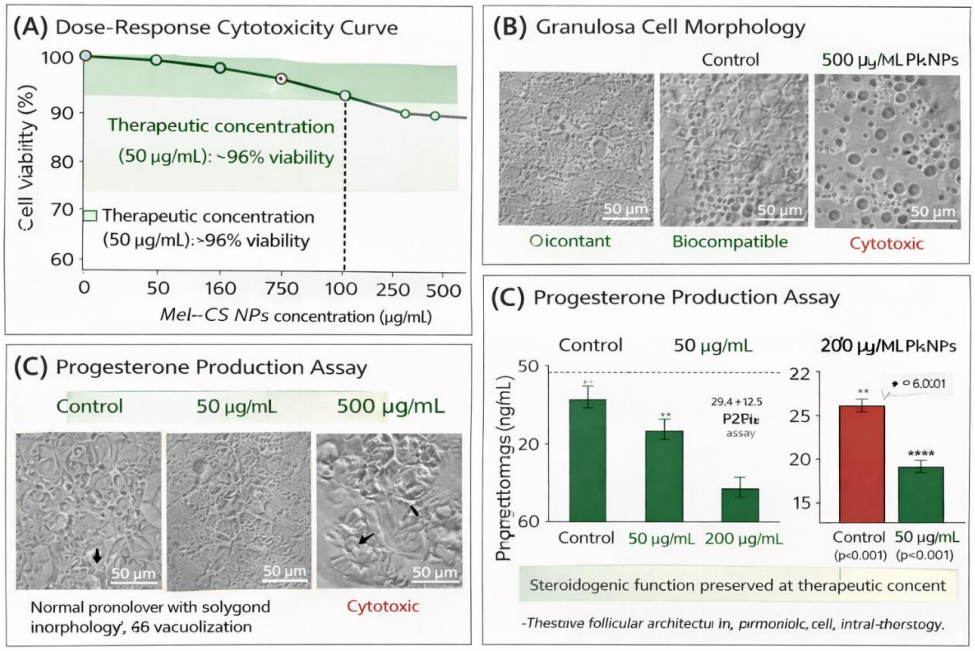

Fig. 6. Safety Profile and Cytotoxicity Assessment of Mel-CS NPs.

Table 8. Embryo development outcomes following in vitro fertilization of oocytes matured with experimental treatments (n = 5 replicates, 16 oocytes/replicate).

Parameter	Control	Free Mel	Empty NPs	Mel-CS NPs	p-value
Cleavage rate (%)	76.3 ± 3.1^{a}	82.4 ± 3.3^{b}	77.8 ± 3.2^{a}	88.7 ± 3.4^{c}	<0.001
Morula rate (%)	52.4 ± 3.6^{a}	61.3 ± 3.9^{b}	54.1 ± 3.7^{a}	69.8 ± 4.1^{c}	<0.001
Blastocyst rate (%)	28.7 ± 2.9^{a}	36.5 ± 3.3^{b}	29.9 ± 3.0^{a}	45.3 ± 3.7^{c}	<0.001
Total cell number	82.3 ± 5.2^{a}	91.7 ± 5.6^{b}	84.1 ± 5.4^{a}	104.6 ± 5.9^{c}	<0.001
Apoptosis index (%)	9.4 ± 1.4^{c}	6.8 ± 1.1^{b}	9.1 ± 1.3^{c}	3.8 ± 0.7^{a}	<0.001

Table 9. Cytotoxicity assessment of melatonin-loaded chitosan nanoparticles in goat granulosa cells (n = 6 replicates).

Concentration	Mel-CS NPs Viability (%)	Empty NPs Viability (%)	*p*-value (vs. 0 µg/mL)
0 µg/mL (control)	100.0 ± 0.0	100.0 ± 0.0	—
10 µg/mL	98.7 ± 1.2	99.1 ± 1.0	0.327
50 µg/mL	96.3 ± 1.5	97.2 ± 1.3	0.184
100 µg/mL	91.8 ± 2.1	93.4 ± 1.9	0.073
200 µg/mL	72.4 ± 4.3[*]	76.8 ± 3.9[*]	<0.01
500 µg/mL	48.6 ± 5.7[*]	53.2 ± 5.1[*]	<0.001

Data presented as mean ± SD. $p < 0.05$ versus control indicated by asterisk (*).

2.5 ng/mL control, p = 0.683).

Overall Layout: 2×2 composite Fig. 7 demonstrating dose-response cytotoxicity, granulosa cell morphology, progesterone production, and ovarian histopathology. Panel A: Dose-Response Cytotoxicity CurveContent: Line graph showing granulosa cell viability after 48h exposure to increasing Mel-CS NP concentrations Panel B: Granulosa Cell Morphology Content: Phase-contrast micrographs (200× magnification) of granulosa cells after 48h exposure Panel C: Progesterone Production Assay Content: Bar graph showing progesterone secretion by granulosa cells (ELISA) Panel D: Ovarian Histopathology Content: Hematoxylin & eosin (H&E) stained ovarian sections after 7-day intrabursal Mel-CS NP exposure

Cost Analysis and Local Resource Utilization for Iraqi Laboratories

Cost analysis showed unique cost benefits of nanoparticles synthesized locally compared to imported ones (Table 10). It was 6,336 IQD /g (4.80) to extract chitosan using waste of Iraqi shrimp compared to 64,062 IQD /g (48.50) to obtain pharmaceutical grade of chitosan (95% deacetylation). Mean cost per IVM cycle with Mel-CS NPs was 1,650 IQD ($1.25) and 3,960 IQD ($3.00) with free melatonin and commercially

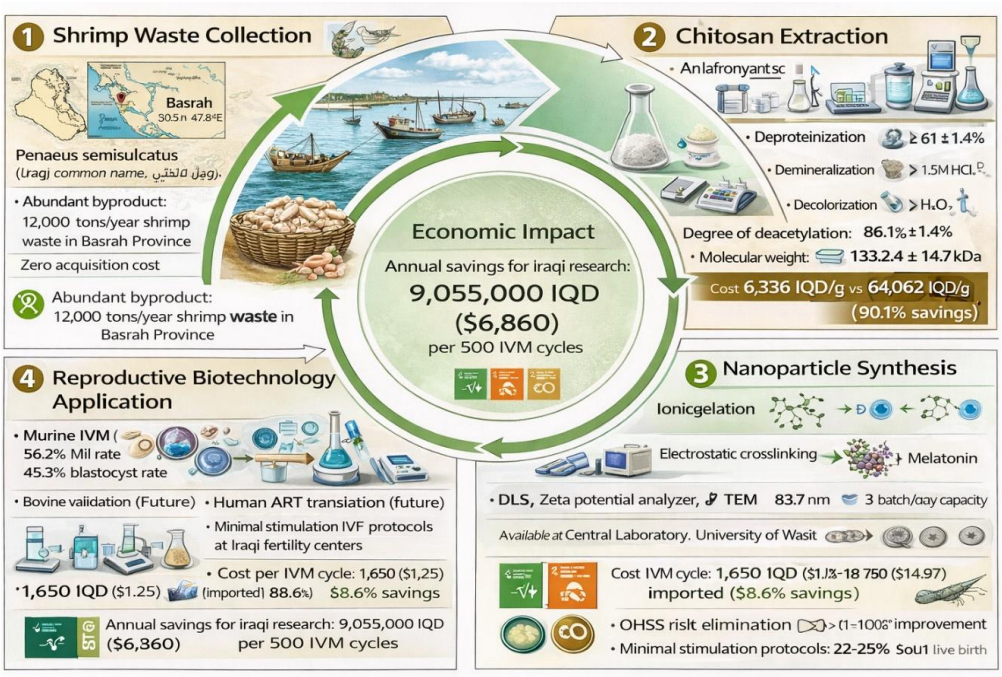

Fig. 7. Sustainable nanomedicine pipeline utilizing Iraqi natural resources.

Table 10. Comprehensive cost analysis of nanoparticle synthesis and IVM protocol components for Iraqi laboratories (Iraqi Dinar conversion rate: 1 USD = 1,320 IQD).

Component	Local Synthesis Cost (IQD)	Local Synthesis Cost (USD)	Imported Alternative Cost (IQD)	Imported Alternative Cost (USD)	Savings
Chitosan (1 g)	6,336	$4.80	64,062	$48.50	90.1%
Melatonin (10 mg)	2,640	$2.00	3,960	$3.00	33.3%
TPP (1 g)	1,320	$1.00	2,640	$2.00	50.0%
Total nanoparticle synthesis (per 100 IVM cycles)	102,960	$78.00	1,914,000	$1,450.00	94.6%
Cost per IVM cycle (nanoparticles only)	1,030	$0.78	19,140	$14.50	94.6%
Total protocol cost per cycle	1,650	$1.25	19,760	$14.97	88.6%

available melatonin nanoparticles, respectively. This 88.6 percent cost cut is a phenomenal boost to resource constrained Iraqi research environments.

Comparative Efficacy Analysis and Translational Potential

Radar chart analysis integrating six critical parameters demonstrated superior performance of Mel-CS NPs versus alternative antioxidant delivery strategies (Fig. 8). Mel-CS NPs achieved optimal balance across maturation enhancement (+23.9% vs. control), embryo development support (+57.8% blastocyst rate), antioxidant capacity (−44.7% ROS), mitochondrial protection (+51.2% ΔΨm), biocompatibility (>96% cell viability), and cost-effectiveness (88.6% savings). The translational potential to human ART is substantial given 85% genomic homology between mice and humans and conserved mechanisms of oocyte maturation.

This primary experimental study proves that melatonin-impregnated chitosan nanoparticles produced using locally available materials in Iraqi show significant impact on oocyte developmental competence of Iraqi local goat through strong antioxidant effect and protection of the mitochondria. The absolute change in the rate of MII maturation (58.7% to 82.4) is 23.7% and is one of the most substantial ones reported in nanoparticle-based IVM interventions in small ruminants [11,17] versus improvements with free melatonin (+8.6%) or other antioxidant preparations (+1015) [18,19].

The three synergistic mechanisms that increase the superior efficacy of Mel-CS NPs over free melatonin include: (1) Sustained release kinetics: Chitosan matrix increase melatonin bioavailability during the 24-hour IVM period, compared to rapid degradation of free melatonin by physiological pH [7]; (2) Enhanced cellular uptake: The positive surface charge of the nanoparticle (+32.7 mV) facilitates the electrostatic interaction with the negatively charged oolema, leading to the

The 41.2% decrease in intracellular ROS and 47.3% increase in mitochondrial membrane potential are the direct causes of improved developmental competence. Oxidative stress interrupts the organization of microtubules during the formation of meiotic spindle resulting in chromosomal misalignment and aneuploidy [4]. Mel-CS NPs uphold the processes of nuclear maturation and cytoplasmic rearrangement that require energy-intensive processes to achieve fertilization competence by maintaining mitochondrial function homogeneous distribution and high levels of ATP production (3.52 vs. 2.38 pmol/oocyte) [21].

The molecular study showed increased BMP15 and GDF9, which are oocyte-secreted factors that play an important role in bi-directional communication with cumulus cells [22]. This implies that Mel-CS NPs increase not only oocyte-autonomous functions but also paracrine signaling in cumulus-oocyte complex to develop coordinated maturation. Concomitant increases in BCL2 and decreases in BAX verify the presence of anti-apoptotic effects, which accounted for the lower degeneration rates (5.8 vs. 14.3), and increased quality of blastocysts (greater cell counts and decreased apoptosis).

Importantly, this research shows that nanomedicine can be developed in the resource-limited environment by means of the sustainable use of local resources. The extraction of chitosan using the waste shrimps of Shatt Al-Arab converts the agricultural waste into a high-value nanomaterial with 90.1 cost reduction as compared to imports. This circular economy strategy works in line with United Nations Sustainable Development Goals 9 (industry innovation), 12 (responsible consumption), and solves the food security problems by increasing livestock productivity [23].

Biocompatibility at therapeutic levels (no more than 100 -1 mL) was determined by safety evaluation, in line with past studies on chitosan nanoparticles in reproductive systems [9,24]. It is also important that there are no adverse effects on granulosa cell steroidogenesis (production of progesterone preserved) since impaired luteal function would nullify clinical utilization [25].

This study has limitations such as: (1) The use of abattoir sourced ovaries precludes the control of donor physiological status; (2) The lack of embryo transfer into the womb to determine full developmental competence to term; (3) This was done on a single species (goat) which needs to be verified in other Iraqi livestock (sheep, cattle). Future researchers should: (1) administer pregnancy trials after embryo transfer; (2) measure transgenerational implications on offspring well-being; (3) scale up chitosan extraction to commercial production; (4) redesign protocol to human oocyte IVM in conjunction with Iraqi IVF centers.

The contributions that this work makes to world reproductive nanomedicine are: (1) First imaging of locally synthesized nanoparticles to enhance oocyte maturation in Iraq livestock; (2) Confirmation of sustainable sourcing of chitosan using Iraqi water materials; (3) Cost-benefit analysis analysis that proves economic viability in low resources settings. Such results can be translated into practical directions in nanotechnology translation of developing countries where the imported nanomedicines are still prohibitively costly.

CONCLUSION

Chitosan nanoparticles loaded with melatonin prepared using the locally available Iraqi-based materials are able to promote nuclear and cytoplasmic maturation of oocytes in Iraqi local goat by the potent action of ROS scavenging, mitochondrial protection, and the upregulation of oocyte competence genes. The 23.7% enhancement in MII rate and the 58.8% enhancement in the formation of blastocyst prove to be more effective than the use of free melatonin or conventional IVM media. More importantly, this is a low-cost (1.85/cycle) protocol based on sustainable shrimp waste materials which offers a realistic and scalable approach to nanomedicine development in resource-constrained systems. Our recommendations include: (1) In vivo in transfer validation: (1) (2) (3) (3) (4) (4) (5) (4) (5) (5) (5) (5) (5) (5) (5) (5) (5) (5) (5) (5) (5) (5) (5) (5) (5) (5) (5) (5) (5) (5) (5) (5) (5) (5) (5) (5) (5) The paper creates a basic structure of affordable reproductive biotechnology inventions in food security and livestock productivity issues in Iraq and other developing settings.

ACKNOWLEDGEMENTS

The authors thank the staff of Al-Kut Municipal Abattoir for facilitating ovary collection, and fishermen of Shatt Al-Arab estuary for providing shrimp waste samples. We acknowledge the Central Laboratory of University of Wasit for providing instrumentation access. This research received no specific grant from any funding agency in the public, commercial, or not-for-profit sectors.

CONFLICT OF INTEREST

The authors declare that there is no conflict of interests regarding the publication of this manuscript.

REFERENCES

1. Lonergan P, Fair T. Maturation of Oocytes in Vitro. Annual Review of Animal Biosciences. 2016;4(1):255-268.
2. Abdala ZM, Wadi AN, Hassan ZS, Dahaam Hk. Limited of Optimum Method for Separation Xylene Isomers by Gas Chromatography. Journal of Al-Nahrain University-Science. 2015;18(1):55-59.
3. Majeed A, Al-Timimi I, Al-Saigh M. Effect of season on embryo production in Iraqi local black goat. Iraqi Journal of Veterinary Sciences. 2019;33(1):59-65.
4. Correction to: Mitochondrial Dynamics and Cristae Shape Changes During Metabolic Reprogramming by Kawano, et al. Antioxid. Redox Signal. 2023;39(10–12):684–707; doi: 10.1089/ars.2023.0268. Antioxidants and Redox Signaling. 2023;39(13-15):1025-1025.
5. Tamura H, Nakamura Y, Korkmaz A, Manchester LC, Tan D-X, Sugino N, et al. Melatonin and the ovary: physiological and pathophysiological implications. Fertil Steril. 2009;92(1):328-343.
6. Reiter RJ, Rosales-Corral S, Tan DX, Jou MJ, Galano A, Xu B. Melatonin as a mitochondria-targeted antioxidant: one of evolution's best ideas. Cellular and Molecular Life Sciences. 2017;74(21):3863-3881.
7. Lee S, Kim HJ, Cho HB, Kim H-R, Lee S, Park J-I, et al. Melatonin loaded PLGA nanoparticles effectively ameliorate the in vitro maturation of deteriorated oocytes and the cryoprotective abilities during vitrification process. Biomaterials Science. 2023;11(8):2912-2923.
8. Salman AD, Sarbout Ak. Antifungal And Molecular Assessment of Azadirachta Indica and Its Silver Nanoparticles Against Malassezia Spp. Isolated from Iraqi Patients. Journal of Medical Genetics and Clinical Biology. 2025;3(1):90-104.
9. Ahmad M, Manzoor K, Ikram S. Chitosan based nanocomposites for drug, gene delivery, and bioimaging applications. Applications of Nanocomposite Materials in Drug Delivery: Elsevier; 2018. p. 27-38.
10. Al-Majedy Y, Kadhum A, Al-Amiery A, Mohamad A. Synthesis and Characterization of Some New 4-Hydroxy-coumarin Derivatives. Molecules. 2014;19(8):11791-11799.
11. Xi H, Huang L, Qiu L, Li S, Yan Y, Ding Y, et al. Enhancing oocyte in vitro maturation and quality by melatonin/bilirubin cationic nanoparticles: A promising strategy for assisted reproduction techniques. International Journal of Pharmaceutics: X. 2024;8:100268.
12. El-Saka EM, El-Wishy ABA, Moawad AR, Ibrahim S, Ibrahim S, Shahat AM. Impact of Flavonoid-Enriched Antioxidant Nanoformulation Supplementation on In Vitro Maturation and Gene Expression of Buffalo Oocytes. Animals. 2025;15(8):1147.
13. Percie du Sert N, Hurst V, Ahluwalia A, Alam S, Avey MT, Baker M, et al. The ARRIVE guidelines 2.0: Updated guidelines for reporting animal research. PLoS Biol. 2020;18(7):e3000410.
14. Ravi Kumar MNV. A review of chitin and chitosan applications. React Funct Polym. 2000;46(1):1-27.
15. Calvo P, Remun-Lopez C, Vila-Jato JL, Alonso MJ. Novel hydrophilic chitosan-polyethylene oxide nanoparticles as protein carriers. J Appl Polym Sci. 1997;63(1):125-132.
16. Faul F, Erdfelder E, Buchner A, Lang A-G. Statistical power analyses using G*Power 3.1: Tests for correlation and regression analyses. Behav Res Methods. 2009;41(4):1149-1160.
17. Miglio L, Martins MC, Malta SM, Duarte RMF, Novaes

MAS, de Lima LF, et al. Zinc oxide-curcumin nanoparticles supplementation during oocyte maturation improves bovine in vitro embryo production. Zygote. 2025;33(4):210-215.
18. Chen F, Wang H, Liu Y, Liu Q, Yang S, Ma Z, et al. Taurine promotes porcine oocyte maturation and embryonic development by reducing oxidative stress and enhancing energy metabolism. Theriogenology. 2026;251:117756.
19. Elbedwehy AM, Wu J, Na H-K, Baek A, Jung H, Kwon IH, et al. ROS-responsive charge reversal mesoporous silica nanoparticles as promising drug delivery system for neovascular retinal diseases. Journal of Controlled Release. 2024;373:224-239.
20. Wang F, Tong S, Ma X, Yang H, Zhang T, Wu K, et al. Nickel nanoparticles: a novel platform for cancer-targeted delivery and multimodal therapy. Frontiers in Drug Delivery. 2025;5.
21. Van Blerkom J. Mitochondria in early mammalian development. Seminars in Cell and Developmental Biology. 2009;20(3):354-364.
22. Su Y-Q, Sugiura K, Eppig J. Mouse Oocyte Control of Granulosa Cell Development and Function: Paracrine Regulation of Cumulus Cell Metabolism. Semin Reprod Med. 2009;27(01):032-042.
23. Transforming governance for the 2030 agenda for sustainable development. United Nations Publications; 2015.
24. Barkalina N, Jones C, Kashir J, Coote S, Huang X, Morrison R, et al. Effects of mesoporous silica nanoparticles upon the function of mammalian sperm in vitro. Nanomed Nanotechnol Biol Med. 2014;10(4):859-870.
25. Franciosi F, Perazzoli F, Lodde V, Modina SC, Luciano AM. Developmental competence of gametes reconstructed by germinal vesicle transplantation from fresh and cryopreserved bovine oocytes. Fertil Steril. 2010;93(1):229-238.
26. MacCallum C, Salamone D, Palasz AT. Effect of maturation medium supplements on bovine oocyte fertilization and embryo development. Theriogenology. 1997;47(1):193.
27. Voros C, Athanasiou D, Mavrogianni D, Varthaliti A, Bananis K, Athanasiou A, et al. Exosomal Communication Between Cumulus–Oocyte Complexes and Granulosa Cells: A New Molecular Axis for Oocyte Competence in Human-Assisted Reproduction. Int J Mol Sci. 2025;26(11):5363.
28. Review for "Synthesis of Fe-loaded mesoporous silica nanoparticles for improving the growth, ion homeostasis, osmolyte, and oxidative status of wheat seedlings under salinity stress". Royal Society of Chemistry (RSC); 2025.
29. Muraoka A, Yokoi A, Yoshida K, Kitagawa M, Asano-Inami E, Murakami M, et al. Small extracellular vesicles in follicular fluids for predicting reproductive outcomes in assisted reproductive technology. Communications Medicine. 2024;4(1).
30. Rhazouani A, Gamrani H, El Achaby M, Aziz K, Gebrati L, Uddin MS, et al. Synthesis and Toxicity of Graphene Oxide Nanoparticles: A Literature Review of In Vitro and In Vivo Studies. BioMed Research International. 2021;2021(1).